Vol. 12, No. 4, 2021
ISSN 2233-4203/ e-ISSN 2093-8950
ARTICLE www.msletters.org | Mass Spectrometry Letters

Fragmentation Analysis of rIAPP Monomer, Dimer, and $[M_{rIAPP} + M_{hIAPP}]^{5+}$ Using Collision-Induced Dissociation with Electrospray Ionization Mass Spectrometry

Jeongmo Kim and Ho-Tae Kim*

Department of Applied Chemistry, Kumoh National Institute of Technology, 61, Daehak-ro, Gumi, Gyeongbuk, Republic of Korea, 39177

Received October 28, 2021; Revised November 12, 2021; Accepted November 25, 2021
First published on the web December 31, 2021; DOI: 10.5478/MSL.2021.12.4.179

Abstract : Collision-induced dissociation (CID) combined with electrospray ionization mass spectrometry (ESI-MS) was used to obtain structural information on rat islet amyloid polypeptide (rIAPP) monomers (M) and dimers (D) observed in the multiply charged state in the MS spectrum. MS/MS analysis indicated that the rIAPP monomers adopt distinct structures depending on the molecular ion charge state. Peptide bond dissociation between L_{27} and P_{28} was observed in the MS/MS spectra of rIAPP monomers, regardless of the monomer molecular ion charge state. MS/MS analysis of the dimers indicated that D^{5+} comprised M^{2+} and M^{3+} subunits, and that the peptide bond dissociation process between the L_{27} and P_{28} residues of the monomer subunit was also maintained. The observation of $(M+ b_{27})^{4+}$ and $(M+ y_{10})^{3+}$ fragment ions were deduced to originate from the two different D^{5+} complex geometries, the N-terminal and C-terminal interaction geometries, respectively. The fragmentation pattern of the $[M_{rIAPP} + M_{hIAPP}]^{5+}$ MS/MS spectrum showed that the interaction occurred between the two N-terminal regions of M_{rIAPP} and M_{hIAPP} in the heterogeneous dimer (hetero-dimer) D^{5+} structure.

Keywords : rat islet amyloid polypeptide (rIAPP), human islet amyloid polypeptide (hIAPP), heterogeneous dimer, collision-induced dissociation mass spectrometry (CID-MS), MS/MS

Introduction

Rat islet amyloid polypeptide (rIAPP), a 37-residue peptide differing from human islet amyloid polypeptide (hIAPP) by six residues in the 18-29 residue region, is known not to form amyloid fibrils.[1,2] Of these 18-29 residues, three are proline residues, which are known to disrupt secondary β-sheet structure formation.[3] rIAPP is thus an example of a natural "β-breaker inhibitor", which prevents the formation and propagation of the β-sheet structure.[4] The rIAPP-based inhibition of hIAPP amyloidogenicity[5-7] or amyloid β aggregation[8] were reported by the formation of rIAPP-hIAPP or rIAPP- amyloid β heterocomplexes.

Amyloid plaques containing aggregates of hIAPP, a 37-residue hormone selectively expressed in pancreatic β-cells, are widely associated with the pathology of type-2-diabetes.[9-11] These fibrillar aggregates are formed via peptide self-assembly into unbranched elongated structures and present filamentous morphology, a cross-β spine, steric zipper structures, and are cytotoxic.[12-14] Recently, there has been much interest in the early oligomerization process of hIAPP because several studies have implicated greater neurotoxicity of smaller prefibrillar hIAPP oligomers over mature fibrils.[15-18] Therefore, it is also important to compare the initial aggregation structure of rIAPP, which does not form amyloid, as a control group, in addition to the analysis of hIAPP early aggregation structures growing to ultimately form amyloid plaques.

Accordingly, there have been several studies on early aggregates of rIAPP. In previous IMS-MS experiments, two different rIAPP D^{5+} conformations were observed based on the arrival time distribution.[19] The Radford group confirmed the gas-phase stability of rIAPP oligomers through CID experiments, demonstrating that they are more stable than hIAPP oligomers.[20] Using solution NMR spectroscopy, Nanga et al. studied the 3D structure of rIAPP in the presence of a membrane and suggested that the α-helix region plays a crucial role in self-association.[1] The structures of rIAPP dimers and oligomers have been studied using molecular dynamics simulations. It was established that the dimer structure of rIAPP is distinct from that of hIAPP because rIAPP displays an α-helix in the N-terminal, with a distortion

*Reprint requests to Ho-Tae Kim
https://orcid.org/0000-0002-1541-3081
E-mail: hotaekim@kumoh.ac.kr

in the middle of the chain, followed by a second shorter α-helix, and is devoid of β-sheets.[21] It was also suggested that rIAPP dimer to pentamer oligomers suffer from marked secondary structural changes due to a significant loss of the C-terminal β-sheet and turn conformation.[22]

Herein, we used CID in conjunction with ESI-MS to obtain structural information on the rIAPP monomer, dimer, and rIAPP-hIAPP hetero-dimer for comparison with the hIAPP dimer structure. The rIAPP homo- or hetero-dimer complexes were allowed to form in solution, and electrosprayed onto a quadrupole ion guide. ESI-MS is assumed to produce intact gas-phase dimer complex ions from the dimer complex in solution. The fragmentation patterns for the rIAPP homo- or hetero-dimer structure were investigated in a 50% H_2O+50% CH_3OH solution. In a previous study, we investigated multiply charged monomers and dimers of hIAPP employing CID-MS/MS.[23]

Experimental

The MS for protein cation complexes and MS/MS spectra for fragmentation pattern analysis were obtained using a Thermo Finnigan LTQ mass spectrometer (Thermo Electron Corp., San Jose, CA, USA), which is a linear ion trap mass spectrometer equipped with an atmospheric pressure-ionization source.

Mass spectrometry conditions

The protein samples were introduced into the electrospray ionization interface via a direct infusion method using a microsyringe pump (Hamilton, USA) at a flow rate of 1–2 mL min^{-1}. The positive ion MS spectra were acquired over an *m/z* range of 700–2000 by averaging 1000–2000 scans. The MS/MS spectra were acquired under the following experimental conditions: activation time of 30 ms, injection time of 100–200 ms, and an isolation width of 1–1.5 mass units. The parent protein ions were individually and manually selected and then subjected to the CID process. The minimal collision energies were optimized for each MS/MS experiment to be viewed at sufficient signal-to-noise ratios.

Reagents

$rIAPP_{1-37}$ and $hIAPP_{1-37}$ (Bachem, Switzerland) were used in the experiments. HPLC-grade H_2O (Merck Ltd., Korea) and HPLC-grade CH_3OH (Merck Ltd., Korea) were used as solvents. The peptides were dissolved in H_2O:CH_3OH (1:1, *v/v*) to prepare 6×10^{-5} M solutions. The solutions were prepared in this manner to achieve sufficient D^{5+} ion intensity in the CID-MS/MS experiments. The experiments were performed within 24 h of sample preparation.

Results and Discussion

MS Spectra

Under the present ESI experimental conditions, the mass spectrum of rIAPP indicated the presence of multiply charged monomers and oligomers (Figure 1). Monomer peaks were observed at *m/z* 1960.0, 1307.0, 980.5, and 784.6, indicating that the monomers had multiple proton adduct charges ranging from 2+ to 5+, [M+2H$^+$] to [M+5H$^+$]. The rIAPP sequence contains three basic residues (Lys1, Arg11, and Arg18) and an N-terminal position available for protonation. Depending on the gas-phase basicity, we

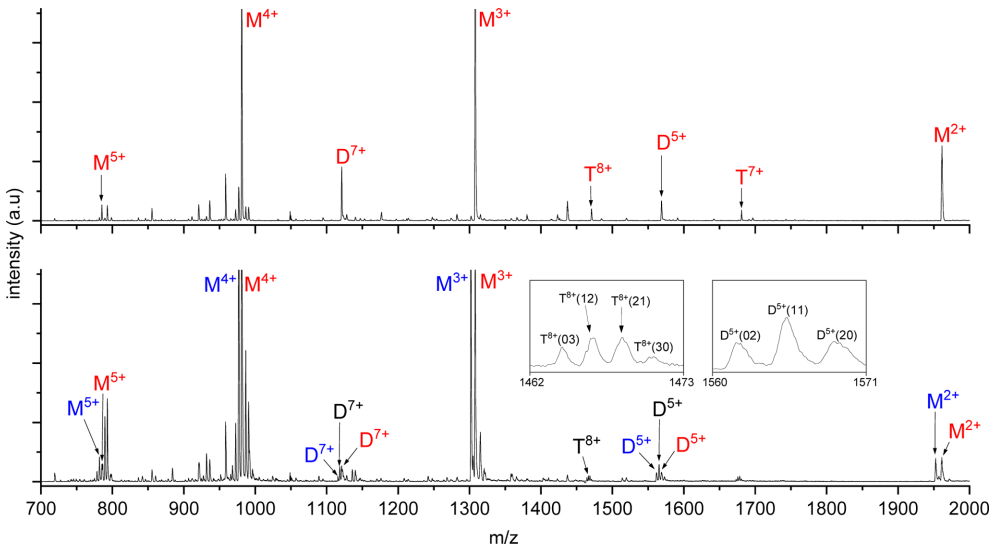

Figure 1. ESI-MS spectrum of (a) rIAPP and (b) rIAPP+hIAPP mixed solution. Multiply charged monomers and oligomers are represented as M^{z+}, D^{z+}, and T^{z+} (M = monomer, D = dimer, T = trimer, and z = charge state). rIAPP and hIAPP are colored red and blue, respectively.

speculate that protonation occurs at Lys1, Arg11, and Arg18 for M^{3+} (*m/z* 1307.0), and at the N-terminal amide for M^{4+} (*m/z* 980.5).[24] Monomers with charges of 3+ and 4+ gave rise to particularly high-intensity peaks. The signal intensity of the M^{5+} (*m/z* 784.6) monomer was lower than that of the other monomer peaks, and it is unclear where the 5th protonation occurs. For the oligomers, peaks were observed at *m/z* 1568.2, 1120.4, 1680.1, and 1470.2, corresponding to D^{5+}, D^{7+}, T^{7+}, and T^{8+} (T = trimer), respectively.

Figure 1b shows the MS spectra of a solution containing the two IAPPs, (rIAPP + hIAPP). The MS spectra of amyloidogenic hIAPP can be found in a previous study.[23] The insets in Figure 1b show enlarged portions of the spectrum containing the signals for the dimers and trimers. The peaks are labeled with their respective (rIAPP: hIAPP) ratios. $D^{5+}(20)$ represents five positive charges of the homo-dimer complex (two rIAPP: zero hIAPP). In Figure 1b, the $D^{5+}(11)$ notation indicates that the hetero-dimer complex is composed of (one rIAPP: one hIAPP) with five positive charges. The $T^{8+}(21)$ notation means that the hetero-trimer complex is composed of (two rIAPP: one hIAPP) with eight positive charges.

In general, the intensities of the homo-dimer and homo-oligomer spectral peaks decreased when the second hetero-IAPP was added to enable the formation of hetero-dimer or hetero-oligomer complexes. In addition to the presence of homo-dimers and homo-trimers, the hetero-dimer $D^{5+}(11)$, hetero-trimer $T^{8+}(21)$, and $T^{8+}(12)$ were also observed as $D^{5+}(20)$, $D^{5+}(02)$, $T^{8+}(30)$, and $T^{8+}(03)$, respectively (Figure 1b). Here, homo-dimer $D^{5+}(02)$ or $D^{5+}(20)$ intensities decreased prominently compared to those shown in Figure 1a and in the previously published spectra.[23] The observed complexes up to their trimer configuration and their *m/z* values are listed in the Electronic Supplementary Information Table S1.

MS/MS Spectra

MS/MS spectra of the monomers

CID-MS/MS experiments were conducted to obtain structural information on the parent rIAPP monomer or dimer ions in the early stages of aggregation. The MS/MS spectra of rIAPP monomers are shown in Figure 2. The fragment ions were labeled with various colors and shapes based on the fragment residue regions to compare the fragmentation patterns of each parent ion. The fragment ion assignments for the spectra in Figure 2 are presented in the Electronic Supplementary Information Table S2.

In the MS/MS spectrum of rIAPP M^{2+} (Figure 2a), we observed three fragment ion series, ① singly charged y_{10}–y_{14} ions, ② doubly charged y_{27}–y_{30} ions, and ③ doubly charged b_{23}–b_{35} fragment ions. The MS/MS fragmentation patterns are presented in Table 1. In the MS/MS spectrum of rIAPP M^{3+} (Fig. 2b), two fragment ion series were observed. Compared to the spectrum of rIAPP M^{2+}, doubly charged y_{27}–y_{30} ions in residues C7–Q10 were not observed in this case (Figure 2b). The dissociation process of residues C7–Q10 was regarded to be hindered because the Arg11 residue is protonated (H^+) depending on the pKa value. The y_{10}–y_{14} ions were commonly observed as singly charged fragment ions, regardless of the monomer charge states (M^{2+}, M^{3+}, and M^{4+}) (Figure 2a–2c). It is worth noting that the b_{27} and y_{10} fragment ions were observed in the spectra shown in Figure 2a–2d as the main dissociation process between L27 and P28.

MS/MS spectra of the dimers

In the CID-MS/MS spectrum of rIAPP D^{5+} (Figure 3a), the fragmentation pattern arising from covalent bond dissociation was observed. Two main fragment ions, $[M+ b_{27}]^{4+}$ and $[M+ y_{10}]^{3+}$, were observed. Those ions are indicating that the peptide bond between L27 and P28 is a critical position in the dissociation process of rIAPP D^{5+}. The $[M+ y_{10}]^{3+}$ is proposed to be a form of $[M^{2+} + y_{10}^{1+}]^{3+}$, based on the observation of y_{10}^{1+} ions (Table 1). The y_{10} ion was always observed in a singly charged state in the MS/MS spectrum of M^{2+}–M^{5+} parent ions. Using the same logic, the b_{27} ion is expected to be in a doubly charged state in the $[M+ b_{27}]^{4+}$ fragment ion. The formation of M^{2+} monomer ion was expected to be conserved in the MS/MS

Table 1. Comparison of MS/MS fragmentation patterns of rIAPP monomers and dimers. The b_u and y_n ions were observed in the fragmentation of monomers, and b_u, y_n, $(M+ b_u)$, and $(M+ y_n)$ were the fragment ions for dimers.

Parent ion	MS/MS fragmentation patterns		
	$[y_{10}]$~$[y_{14}]$	$[y_{27}]$~$[y_{30}]$	$[b_{23}]$~$[b_{35}]$
M^{2+}	1+	2+	2+
M^{3+}	1+	N/A	2+
M^{4+}	1+	N/A	2+,3+
M^{5+}	1+	N/A	3+,4+
rIAPP D^{5+}	y_{10}^{1+}	N/A	$[M+b_{23}]^{4+} \sim [M+b_{34}]^{4+}$
	$[M+y_{10}]^{3+}$, $[M+y_{11}]^{3+}$	N/A	$b_{23}^{2+} \sim b_{27}^{2+}$
Hetero- D^{5+}	$rat{:}y_{10}^{1+} \sim rat{:}y_{14}^{1+}$	N/A	$[M_h+rat{:}b_{23}]^{4+} \sim [M_h+rat{:}b_{27}]^{4+}$ $[M_r+human{:}b_{23}]^{4+} \sim [M_r+human{:}b_{35}]^{4+}$

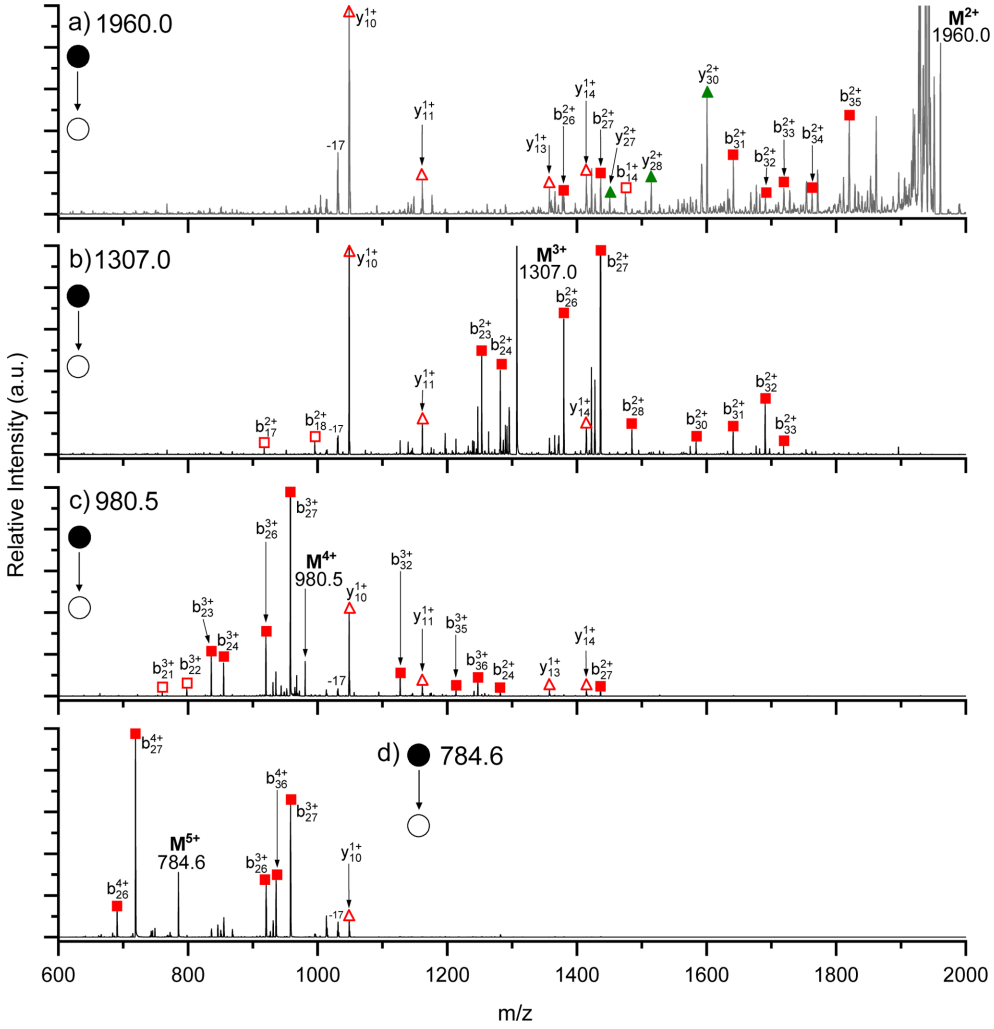

Figure 2. MS/MS spectra of monomers of rIAPP (a) M^{2+}, (b) M^{3+}, (c) M^{4+}, (d) M^{5+}. The b_u fragment series peak at u = 23–35 is indicated by a red square at the top of the peak and the y_n fragment series peaks at u = 10–14 and u = 27–30 are indicated by red and green triangles, respectively.

dissociation process of rIAPP D^{5+}. In other words, the fragmentation process was expected to occur in the M^{3+} monomer form in the MS/MS of rIAPP D^{5+}. Therefore, the parent ion rIAPP D^{5+} is surmised to be composed of M^{2+} and M^{3+}. As further evidence, in the CID-MS/MS experiments with broader mass isolation widths, it was observed that all of the rIAPP D^{5+} parent ions dissociated into M^{2+} (*m/z* 1960) and M^{3+} (*m/z* 1307) (Figure S1).

The two proposed rIAPP D^{5+} structures are shown in Scheme 1, based on the observation of $(M+ b_{27})^{4+}$ and $(M+ y_{10})^{3+}$ fragment ions. We postulate the coexistence of the two proposed configurations of D^{5+} (Scheme 1a and 1b) in the rIAPP solution. The coexistence of two rIAPP D^{5+} geometries could be a possible explanation for the observation of two peaks in the IMS-MS spectrum of rIAPP D^{5+}.[19]

The observation of $(M+ b_u)^{4+}$ fragment ion series, u = 23−34, suggests dimer interactions at the 1−22 residue region (Scheme 1a); this spectrum is consistent with dimer structures involving N-terminal helix-helix interactions, as shown in previous hIAPP studies.[25] A significant contribution from the L12−L12 and F15−F15 interactions between the monomers has also been reported.[26] The observation of $(M + b_u)^{4+}$ fragment ion series, u = 23−34, could not provide insight into whether the hIAPP 1–22 region forms a helical coil or not. Nonetheless, the observation of the $(M + b_u)^{4+}$ series (u = 23−34) did indicate the presence of interactions in the 1–22 residue region, where the dissociation process of the dimer complex is expected to be hindered. The assumption of these 1−22 domain interactions between two rIAPP molecules was supported by the observation of the $(b_{27} + b_{27})^{4+}$ fragment ion in the MS/MS/MS spectrum of the $(M+ b_{27})^{4+}$ parent ion (Figure S2).

The observation of the $(M+ y_{10})^{3+}$ and b_u^{2+} series (u =

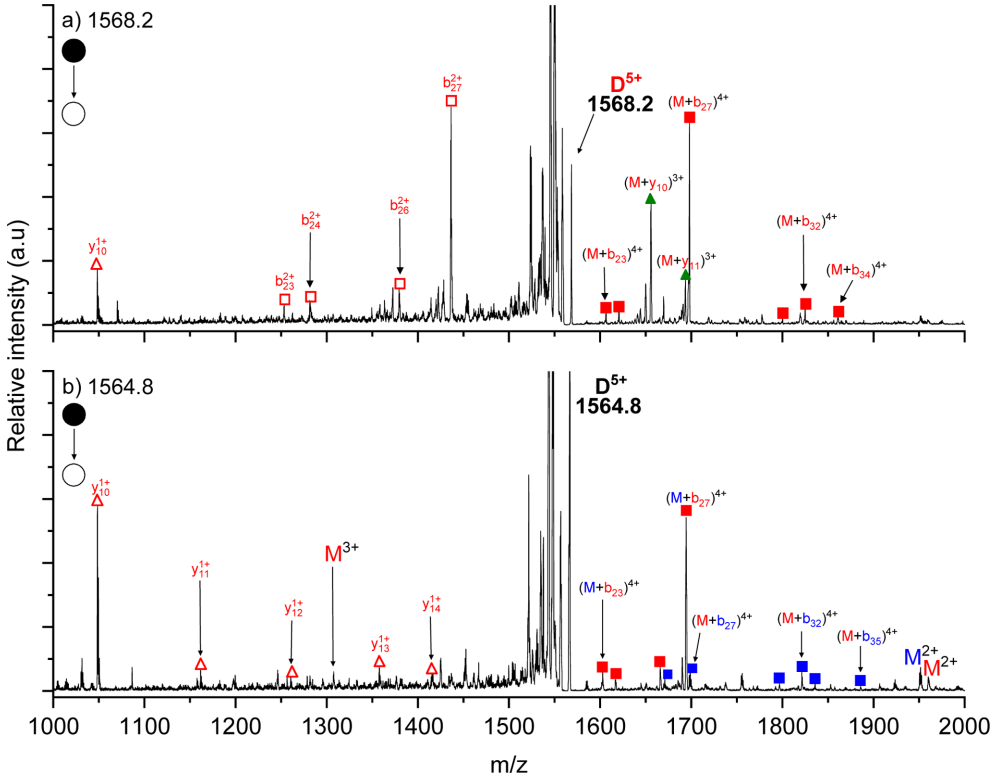

Figure 3. MS/MS spectrum of (a) rIAPP D^{5+} dimer and (b) hetero-D^{5+} .$[M+ b_u]^{4+}$ fragment series peaks at u = 23–34 are indicated by a red square at the top of the peak and the $(M+ y_n)^{3+}$ and y_n fragment series peaks at n = 10–14 are indicated by red and green triangles, respectively. rIAPP and hIAPP are indicated in red and blue, respectively.

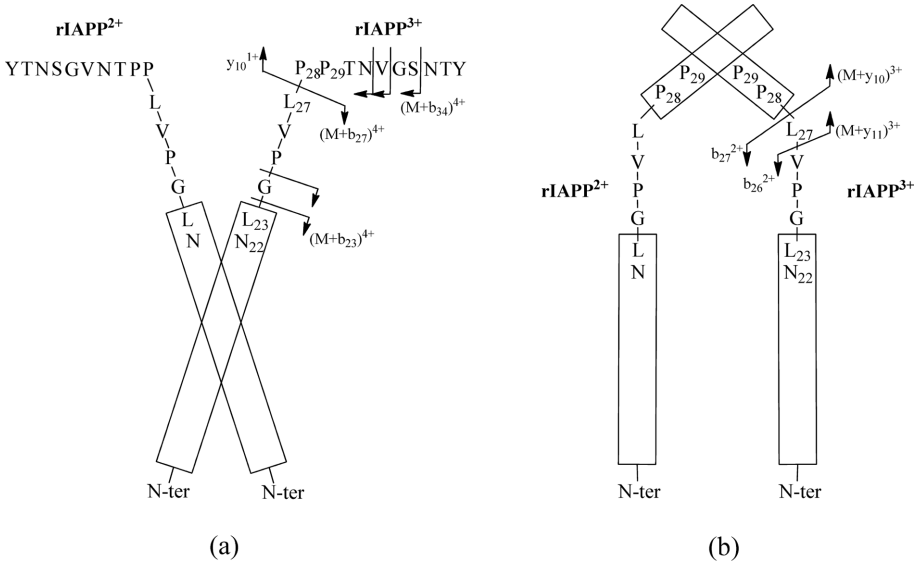

Scheme 1. Schematic diagram of the proposed rIAPP D^{5+}structures.

23−27) in Figure 3a is inconsistent with the geometry shown in Scheme 1a. These observations suggest another dimer interaction at the 28−37 region (Scheme 1b), which is incompatible with the geometry shown in Scheme 1a. The dimer interaction in the 28−37 region has been proposed to occur in β-strand interactions between β-hairpin monomers[19,27] and in the disordered loop region of the monomers,[28] in which the C-terminal or 28–37 residue

region is not amenable to the CID dissociation process. The inference of these C-terminal or 28–37 domains interaction between two rIAPP molecules was supported by the observation of the b_u^{2+} series (u = 23−27) and the absence of the b_u^{2+} ions in the 28–37 residues in the MS/MS/MS spectrum of the $(M+ y_{10})^{3+}$ parent ion (Figure S2).

The covalent and non-covalent bond dissociation was observed in the CID-MS/MS spectrum of rIAPP-hIAPP hetero-dimer $D^{5+}(11)$ parent ions (Figure 3b). Three monomer fragment ions ($rIAPP^{2+}$, $rIAPP^{3+}$, and $hIAPP^{2+}$) were observed as products of the non-covalent bond dissociation process of the hetero-dimer $D^{5+}(11)$ complex. It is assumed that the $D^{5+}(11)$ complex comprises two possible hetero-dimer structures, ($rIAPP^{3+}$ + $hIAPP^{2+}$) or ($rIAPP^{2+}$ + $hIAPP^{3+}$). The formation of the ($rIAPP^{3+}$ + $hIAPP^{2+}$) complex was supported by the observation of ($hIAPP^{2+}$ + rIAPP: b_{23}–b_{27} ions)$^{4+}$ and (rIAPP: y_{10}–y_{14} ions)$^{1+}$ fragment ions in the spectrum of Fig. 3b. The formation of the ($rIAPP^{2+}$ + $hIAPP^{3+}$) structure was supported by the observation of the ($rIAPP^{2+}$ + hIAPP: b_u)$^{4+}$ fragment series from u = 26 to u = 35, which implies an interaction between $hIAPP^{2+}$ and the 1−22 residue region of $rIAPP^{3+}$. The fragmentation process was expected to occur in the 3+ monomer charge state, $rIAPP^{3+}$ in ($rIAPP^{3+}$ + $hIAPP^{2+}$), and $hIAPP^{3+}$ in the ($rIAPP^{2+}$ + $hIAPP^{3+}$) complex. It is worth noting that the absence of ($hIAPP^{2+}$ + rIAPP: y_{10})$^{3+}$ distinguishes the rIAPP-hIAPP hetero-dimer spectrum from the rIAPP homo-dimer MS/MS spectrum in Figure 3a.

Therefore, the ($hIAPP^{2+}$ + $rIAPP^{3+}$) hetero-dimer geometry is expected to be similar to that of the Scheme 1a structure, wherein N-terminal domain interaction was proposed for the rIAPP homo-dimer or hIAPP homo-dimer in previous studies.[23] The proposed N-terminal domain interaction structure appears to be consistent with the 2D IR experimental results at 24 h after mixing rIAPP and hIAPP.[6] Both the observed ($rIAPP^{2+}$ + hIAPP:$b_{26\text{-}35}$)$^{4+}$ fragment ions and the absence of ($hIAPP^{2+}$ + rIAPP: y_{10})$^{3+}$ implied that the C-terminal domain interaction geometry, which is similar to that of the structure in Scheme 1b, is not favorable in the hetero-dimer $2^{5+}(11)$ complex.

Conclusion

CID-MS/MS experiments were conducted to obtain structural information on the monomers and dimers formed in the early stages of rIAPP aggregation. The MS/MS spectra of the rIAPP monomers showed that there were two different fragmentation patterns, (M^{2+} fragmentation pattern) and (M^{3+}, M^{4+} and M^{5+} fragmentation pattern), indicating that the rIAPP monomer structures depend on the charge state of parent monomer ion. Non-covalent or covalent bond dissociation was observed in the MS/MS spectra of $[M_{rIAPP} + M_{rIAPP}]^{5+}$ or $[M_{rIAPP} + M_{hIAPP}]^{5+}$. The fragment ions of $[M_{rIAPP} + M_{hIAPP}]^{5+}$ for the non-covalent bond dissociation process, M^{2+} and M^{3+}, indicated that $[M_{rIAPP} + M_{hIAPP}]^{5+}$ hetero-dimer was composed of M^{2+} and M^{3+} monomers. The covalent bond dissociation patterns corresponding to $(M+ b_{27})^{4+}$ and $(M+ y_{10})^{3+}$ indicated the co-existence of two rIAPP D^{5+} configurations, proposed in Schemes 1a and 1b, in the rIAPP solution. The observation of ($hIAPP^{2+}$ + rIAPP: b_{27})$^{4+}$ and ($rIAPP^{2+}$ + hIAPP: b_{27})$^{4+}$ in the MS/MS spectrum of $[M_{rIAPP} + M_{hIAPP}]^{5+}$ hetero-dimer indicated that the geometry of Scheme 1a complex was favorable in the hetero-dimer complex structure.

Supplementary Information

Supplementary information is available at https://docs.google.com/document/d/1h9Lcp7xR3woZtmWzfoMJTQ5Qoo80gJ2c/edit?usp=sharing&ouid=111353140014732050956&rtpof=true&sd=true.

Acknowledgments

This paper was supported by Research Fund, Kumoh National Institute of Technology (2019-104-061).

References

1. Nanga, R. P. R.; Brender, J. R.; Xu, J.; Hartman, K.; Subramanian, V.; and Ramamoorthy, A. *J. Am. Chem. Soc.* **2019**, 131, 8252, DOI: 10.1021/ja9010095.
2. Green, J.; Goldsbury, C.; Mini, T.; Sunderji, S.; Frey, P.; Kistler, J.; Cooper, G.; Aebi, U. *J. Mol. Biol*. **2003**, 326, 1147, DOI: 10.1016/S0022-2836(02)01377-3.
3. Chiu, C.-C.; de Pablo J. J. *AIP Adv.* **2015**, 5, 092501, DOI: 10.1063/1.4921073.
4. Wang, H.; Ridgway, Z.; Cao, P.; Ruzsicska, B.; Raleigh, D. P. *Biochemistry* **2015**, 54, 6704, DOI: 10.1021/acs.biochem.5b00567.
5. Sellin, D.; Yan, L.-M.; Kapurniotu, A.; Winter, R. *Biophys. Chem*. **2010**, 150, 73, DOI: 10.1016/j.bpc.2010.01.006.
6. Middleton, C. T.; Marek, P.; Cao, P.; Chiu, C.-C.; Singh, S.; Woys, A. M.; de Pablo, J. J.; Raleigh, D. P.; Zanni, M. T. *Nat. Chem*. **2012**, 4, 355, DOI: 10.1038/NCHEM.1293.
7. Cao, P.; Meng, F.; Abedini, A.; Raleigh, D. P. *Biochemistry* **2010**, 49, 872, DOI: 10.1021/bi901751b.
8. Bharadwaj, P.; Solomon, T.; Sahoo, B. R.; Ignasiak, K.; Gaskin, S.; Rowles, J.; Verdile, G.; Howard, M. J.; Bond, C. S.; Ramamoorthy, A.; Martins, R. N.; Newsholme, P. *Sci. Rep*. **2020**, 10, 10356, DOI: 10.1038/s41598-020-66602-9.
9. Cooper, G. J. S.; Willis, A. C.; Clark, A.; Turner, R. C.; Sim, R. B.; Reid, K. B. M. *Proc. Natl. Acad. Sci. USA*. **1987**, 84, 8628, DOI: 10.1073/pnas.84.23.8628.
10. Hoppener, J. W.; Lips, C. J. *Int. J. Biochem. Cell Biol.* **2006**, 38, 726, DOI: 10.1016/j.biocel.2005.12.009.
11. Guo, J.; Sun, W.; Li, L.; Liu, F.; Lu, W. *RSC Adv.* **2017**, 7,

43491, DOI: 10.1039/C7RA05742C.
12. Nelson, R.; Sawaya, M. R.; Balbirnie, M.; Madsen, A. O.; Riekel, C.; Grothe, R.; Eisenberg, D. *Nature*. **2005**, 435, 773, DOI: 10.1038/nature03680.
13. Sawaya, M. R.; Sambashivan, S.; Nelson, R.; Ivanova, M. I.; Sievers, S. A.; Apostol, M. I.; Thompson, M. J.; Balbirnie, M.; Wiltzius, J. J.; McFarlane, H. T.; Madsen, A.; Riekel, C.; Eisenberg, D. *Nature* **2007**, 447, 453, DOI: 10.1038/nature05695.
14. Jobling, M. F.; Stewart, L. R.; White, A. R.; McLean, C.; Friedhuber, A.; Maher, F.; Beyreuther, K.; Masters, C. L.; Barrow, C. J.; Collins, S. J.; Cappai, R. *J. Neurochem.* **1999**, 73, 1557 DOI: 10.1046/j.1471-4159.1999.0731557.x.
15. Haataja, L.; Gurlo, T.; Huang, C. J.; Butler, P. C. *Endocr. Rev.* **2008**, 29, 303, DOI: 10.1210/er.2007-0037.
16. Hebda, J. A.; Miranker, A. D. *Annu. Rev. Biophys.* **2009**, 38, 125, DOI: 10.1146/annurev.biophys.050708.133622.
17. Lin, C. Y.; Gurlo, T.; Kayed, R.; Butler, A. E.; Haataja, L.; Glabe, C. G.; Butler, P. C. *Diabetes* **2007**, 56, 1324, DOI: 10.2337/db06-1579.
18. Liu, N.; Duan, M.; Yang, M. *Sci. Rep.* **2017**, 7, 7915, DOI: 10.1038/s41598-017-08504-x.
19. Dupuis, N. F.; Wu, C.; Shea, J.-E.; Bowers, M. T. *J. Am. Chem. Soc.* **2011**, 133, 7240, DOI: 10.1021/ja1081537.
20. Young, L. M.; Cao, P.; Raleigh, D. P.; Ashcroft, A. E.; Radford, S. E. *J. Am. Chem. Soc.* **2014**, 136, 660, DOI: 10.1021/ja406831n.
21. Laghaei, R.; Mousseau, N.; Wei, G. H. *J. Phys. Chem. B.* 2011, 115, 3146, DOI: 10.1021/jp108870q.
22. Liang, G.; Zhao, J.; Yu, X.; Zheng, J. *Biochemistry* **2013**, 52, 1089, DOI: 10.1021/bi301525e.
23. Seo, J.-H.; Cha, E.; Kim, H.-T. *Chem. Phys. Lett.* **2018**, 708, 61, DOI: 10.1016/j.cplett.2019.06.044.
24. Dupuis, N. F.; Wu, C.; Shea, J. E.; Bowers, M. T. *J. Am. Chem. Soc.* **2009**, 131, 18283, DOI: 10.1021/ja903814q.
25. Wiltzius, J. J. W.; Sievers, S. A.; Sawaya, M. R.; Eisenberg, D. *Protein Sci*. **2009**, 18, 1521, DOI: 10.1002/pro.145.
26. Zhao, D. S.; Chen, Y. X.; Li, Y. M. *Chem. Commun.* **2015**, 51, 2095, DOI: 10.1039/c4cc06739h.
27. Mo, Y.; Lei, J.; Sun, Y.; Zhang, Q.; Wei, G. *Sci. Rep.* **2016**, 6, 33076, DOI: 10.1038/srep33076.
28. Buchanan, L. E.; Dunkelberger, E. B.; Tran, H. Q.; Cheng, P. N.; Chiu, C. C.; Cao, P.; Raleigh, D. P.; de Pablo, J. J.; Nowick, J. S.; Zanni, M. T. *Proc. Natl. Acad. Sci. USA* **2013**, 110, 19285, DOI: 10.1073/pnas.1314481110.